Book Section:
Ayala, G., Wainwright, J., Lloyd, J.M. et al. (2021) Disentangling the palaeoenvironmental reconstructions of Çatalhöyük. In: Hodder, I., (ed.) Peopling the landscape of Çatalhöyük: Reports from the 2009-2017 Seasons. Çatalhöyük Research Project Series, 13. British Institute at Ankara, pp. 31-46. ISBN: 9781912090785.

2. Disentangling the palaeoenvironmental reconstructions of Çatalhöyük

Gianna Ayala, John Wainwright, Jerry M. Lloyd, Joanna R. Walker, Rachel Hodara Nelson, Melanie Leng, Chris Doherty and Michael Charles

Introduction

This chapter focuses on the ongoing landscape investigations in the immediate vicinity of the two tell sites at Çatalhöyük, concentrating on how the natural world shaped peoples' engagement with their environment. The chapter builds upon a long history of environmental research in the region, not just at Çatalhöyük (Roberts 1991; 1995; Roberts et al. 1996; 1999; Rosen, Roberts 2005; Roberts, Rosen 2009) but more widely in the Konya Plain (Boyer 1999: 63; Boyer et al. 2006: 684; Boyer et al. 2007; Roberts et al. 2016).

There are two main aims of this chapter. Our first aim is to evaluate previous palaeoenvironmental models and refine them with additional and enhanced datasets from the current programme of landscape research (with field sampling from 2007–2015). The focus of our study has therefore been the high-resolution palaeoenvironmental reconstruction of the alluvial landscape in the vicinity of the site. The modern Çarşamba River flows close to the edge of the site and extends southwards until the termination of the Konya Plain at the limestone hills that border the Taurus Mountains (fig. 2.1). However, the river historically had a branch which flowed between the East and West Mounds. Previous geoarchaeological research has characterised the alluvial plain as a very marshy environment subject to significant seasonal flooding (Roberts et al. 1999; Rosen, Roberts 2005; Boyer et al. 2006; Roberts, Rosen 2009), which was based on sedimentological data derived from nine coring locations and trench sections near the tells as well as the investigation of 16 archaeological sites (four of which date from the Palaeolithic to Bronze Age) further away in the area of the Konya palaeolake (Boyer 1999: 63; Boyer et al. 2006: 684; Boyer et al. 2007).

In this chapter we present the recent programme of research (Ayala et al. 2017) and describe how the current palaeohydrological model we propose has been constructed. The evidence comes from a coring programme undertaken between 2007 and 2015 that targeted 29 coring locations within a radius of up to 1.6km of Çatalhöyük using both more intensive and more extensive sampling protocols than previously utilised in this region (fig. 2.1). A combination of sediment and isotope analysis, and 3D modelling of the stratigraphic sequence has enabled us to construct a more refined understanding of the hydrology and resulting dynamic topography of the low-lying alluvial plain (Ayala et al. 2017). After summarising the results from Ayala et al. 2017, we show how an additional 34 cores taken in 2015 allow us to refine the palaeoenvironmental model further. Pollen and isotope data are used to evaluate the broader landscape and climate context of the site. We also reinterpret the existing hydrological data used as a basis for the spring-flooding hypothesis and demonstrate that its use is highly problematic.

The second aim of the chapter is to highlight how the new geoarchaeological data not only enhance and refine the previous landscape models of the region, but importantly support new ways of thinking about the archaeological record. Our research presents a narrative of landscape formation that is fundamental for any interpretation of how people at Çatalhöyük were entwined with their world, both constrained by the very physicality of the environment and transforming the matter and substances within which they were entangled. Hodder has highlighted the experiences and processes which became part of daily life, from construction of structures to the domestication of foodstuffs, as a complex and dynamic relationship interlacing the materiality of human existence with the environment (Hodder 2011: 160–62; Hodder 2012). Through this understanding of human-thing relationships, people's entanglements with environmental processes have been regarded as a driving force for change and adaption (Hodder 2011).

Our understanding of these processes and behavioural reactions is dependent on accurate and high-resolution reconstruction of environmental parameters. Excavation and off-site investigations at Çatalhöyük have provided intriguing evidence that has been used to suggest lines of this entangled relationship (Roberts et al. 2007; Roberts, Rosen 2009; Love 2012; Charles et al. 2014; Doherty 2017). The classic example of an entangled environment-thing relationship based on one

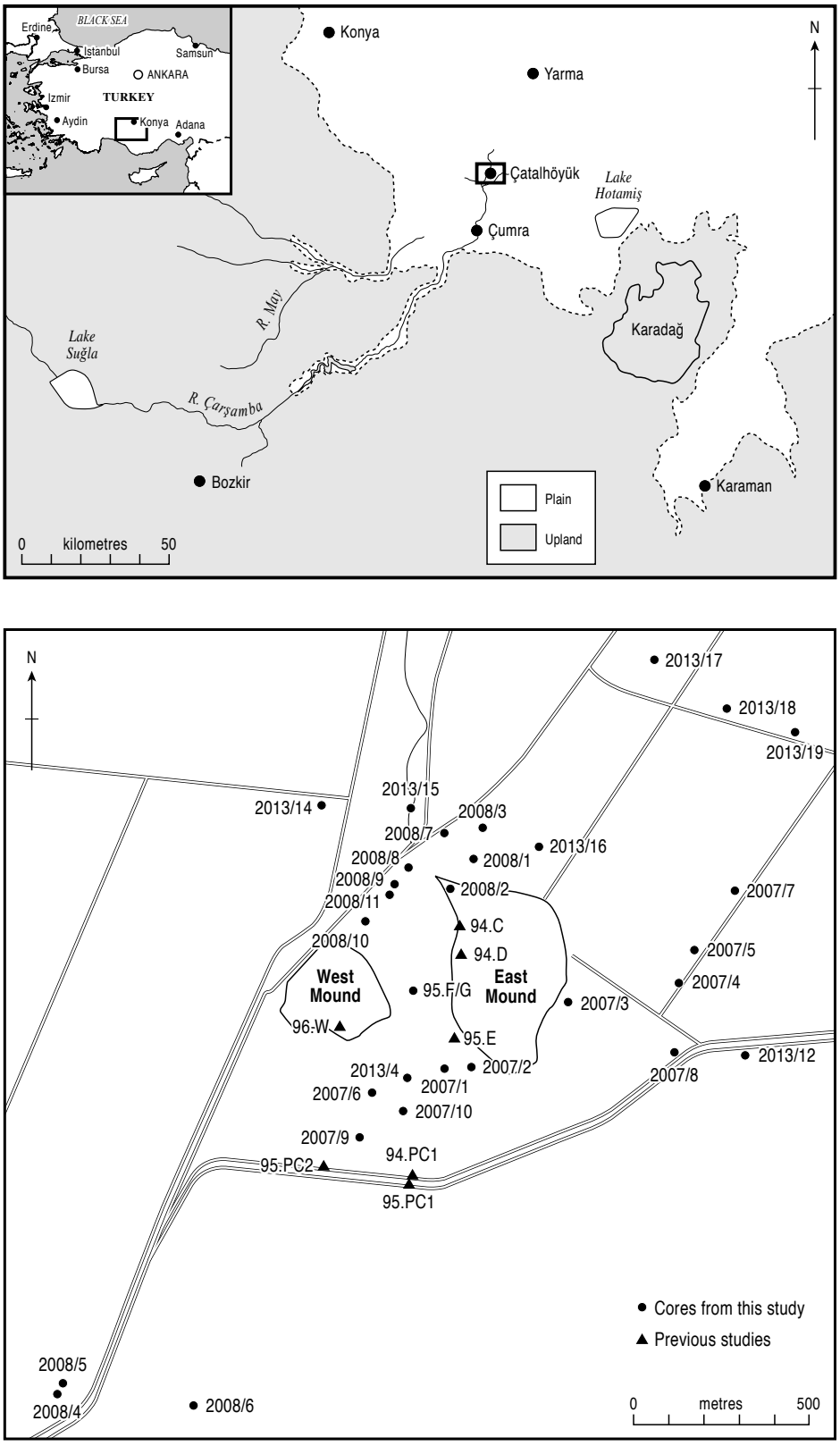

Figure 2.1. Location of site and coring locations (KOPAL and 2007–2013) (Ayala et al. 2017: fig. 1). See fig. 2.4 for additional cores taken in 2015.

of these paleoenvironmental reconstructions is the identification of depressions near the East Mound which have been interpreted as clay extraction pits for the production of clay bricks (Roberts et al. 2007; Hodder 2011: 161–62). These depressions reach the marl sediment underlying the alluvium. Archaeometric analysis of plaster and mudbrick from the site has identified marl as a key constituent in the earliest occupation levels (Love 2012; Doherty 2017). The creation of the pits has been attributed to the occupants' search for appropriate building material in the earliest habitation phases. The pits have also been attributed with providing the perfect damp conditions that would have encouraged the spread of invasive wetland vegetation. It has been suggested that the extraction of clay for building material and the invasion of wetland plant species affected the local topography and hydrology surrounding the site (Charles et al. 2014: 86; Philippa Ryan cited in Hodder 2011). These interpretations are clearly interdependent on the reconstruction of the type of river system near the site and its flood regime, as well as the interpretation of features such as these depressions in the underlying marl near the tell (Charles et al. 2014; Doherty 2017).

The importance of a high-resolution reconstruction of the palaeoenvironment in the vicinity of the settlement becomes increasingly greater as we attempt to interpret behavioural patterns and choices that were open to and taken by the occupants of Çatalhöyük. Previous attempts to reconstruct land-use patterns or 'taskscapes' of Çatalhöyük have been based on environmental proxies (Roberts, Rosen 2009; Bogaard et al. 2014a; Charles et al. 2014; Bogaard et al. 2017). To investigate more closely one of the most fundamental environmental parameters key to the raft of human-thing relationships, namely water, a programme of intensive coring was undertaken in the vicinity of the tell (Ayala et al. 2017) to define the morphology and development of the palaeo-Çarşamba River. This research is designed to feed into the multitude of ways in which the materiality of the archaeological record can be interpreted in relation to the environmental record. It is hoped that with an accurate model of the development of the alluvial landscape surrounding Çatalhöyük we will be able to enhance the interpretations of issues including but not limited to resource provision, the mapping of seasonal tasks, and the development and evolution of agriculture and animal husbandry, as well as the construction and maintenance of the tell itself (Doherty 2017) and the lifeways within.

In the first section of this chapter we review the previous palaeoenvironmental work undertaken at the site and within the Konya Plain. From this basis we assess the reconstruction of the palaeolandscape from this evidence and the implications it had for previous land-use models. We then present the findings to date from the recent programme of coring, followed by a discussion of the evidence and reinterpretation of the palaeohydrology on the alluvial plain upon which the site is located. Finally, we present future goals and directions for the project.

Palaeoenvironmental context

Previous palaeoenvironmental research in the Konya Basin

Çatalhöyük is located in the southern part of the Konya Basin, which is a closed pluvial basin. The present course of the Çarşamba River is to the west of Çatalhöyük, but it has been diverted over the last 50 years and is currently constrained by a concrete channel. Previously it would have had much more ability to move across the low-angled fan surface, after its debouchment from the constrained upland section south of Çumra, and through the sand ridge (a palaeolake shoreline) north of Çumra. Evidence from the past century suggests that in recent historical times, the Çarşamba flowed in a single-thread channel between the East and West Mounds (Rosen, Roberts 2005; Roberts, Rosen 2009).

Early studies of the palaeoenvironment were carried out by the pedologist de Meester (1970: 86), who considered that that the Neolithic soils were formed under 'semi-lacustrine marsh' conditions in a deltaic context. The KOPAL (KOnya basin PALaeoenvironmental research) project concurred with de Meester's (1970) assessment of soil formation. Roberts et al. (1999) defined three broad sets of deposit: (i) a dark, organic clay deposit interpreted as a marsh or backswamp deposit; (ii) the 'Lower Alluvium' made up of dark-grey-brown silt-clay representing a seasonally flooding environment; and (iii) the 'Upper Alluvium', which has a slightly coarser grain size and increased carbonate content. The first of these deposits was interpreted (ibid.: 624) as forming just before settlement of Neolithic Çatalhöyük (ca 7400 cal BCE: Bayliss et al. 2015), the second as being contemporaneous with the occupation of Çatalhöyük (from ca 7000 cal BCE) (Roberts et al. 1999: 625), and the third at some point in the mid-Holocene (ibid.: 627). Roberts and Rosen (2009) asserted that the shift to the Upper Alluvium represented a reduction in alluvial flooding that correlated with the 8.2kya event that is, ca 6250 cal BCE), which is seen in Greenland ice cores (Gasse 2000; Alley, Ágústsdóttir 2005), even though this shift is very poorly dated locally. We will return to the interpretation of the 8.2kya event in the section on palaeoenvironmental proxies.

Despite the previous, extensive work carried out in the Konya Basin, the current palaeoenvironmental reassessment was driven forward by the perspective that previous approaches have tended not to recognise the

inherent heterogeneity of dryland environments (Parsons, Abrahams 2009; Müller et al. 2013). Spatial heterogeneity is reinforced by temporal variability in Mediterranean climates (Wainwright, Thornes 2004). Small samples in space and time are therefore problematic when reconstructing dynamic landscape change, which seems to have been the case for Neolithic Çatalhöyük. Thus, the present study has started to focus on more intensive, detailed approaches to sampling and reconstruction.

The 2007–2013 field seasons

Recovery and laboratory methods. A total of 29 sediment cores from different coring locations were taken in 2007–2013 (fig. 2.1). These were focused on the immediate environment surrounding the two tells. In the first instance, the coring programme of 2007–2008 concentrated on an area within 1km of the site, with coring locations spread out in order to ensure representation of potentially varied microenvironments. All cores were extracted with a percussion corer. The cores in 2007 were taken in discontinuous 0.5m sections, while in 2008 a system of coring parallel sets of overlapping cores 1–2m apart was employed to ensure that a continuous sequence was recovered. Cores were taken from 21 different locations roughly following east/west transects. The cores went to a depth of 3 to 5m and were extracted in 0.5m sections which were then described and photographed in the field, wrapped in cellophane and placed in plastic guttering for transportation back to the UK, where they were refrigerated prior to analysis. Subsampling for sediment was carried out at 0.05m intervals on the 2007 cores, while sampling was focused on the identified lithological units on 2008 and 2013 cores. The second set of cores in this set were taken in the summer of 2013, a further eight coring locations were sampled from an area ca 2km^2 centred around the Çatalhöyük settlement mounds, using transects that concentrated on areas that had not previously been sampled. At each location a parallel set of overlapping cores was taken 2–3m apart to a depth of 5m (8 × 4.50m from each borehole; the top 0.5m was discarded due to considerable modern reworking of sediments by agriculture since the Hellenistic-Byzantine period) (Boyer et al. 2006). Following transportation, all cores were then refrigerated to prevent degradation before analysis (Tirlea et al. 2014). The lithology of the cores was studied, and colour, sediment type and grain size were recorded (Melville, Atkinson 1985; Munsell Color Company 1994). Sediment analyses included magnetic susceptibility, loss on ignition, particle size and isotope analysis (Ayala et al. 2017). These observations were then mapped and plotted using RockWorks™ v16 software.

Results. The analysis of the cores allowed us to identify the stratigraphy shown in figure 2.2. Based on this evidence, we determined sediment complexes and plotted this stratigraphical information as a fence diagram, revealing the distribution of the subsurface sequence in the environs of the two tells (fig. 2.3).

The Basal Complex. The lowest part of the sequence is made up of marl, and sands with gravel in units of 0.1–0.5m thickness. The sands and gravels tend to be moderately to well sorted, all subrounded to rounded. Poorly sorted layers are present locally and tend to be constituted by mixed granules of different lithologies derived from the local limestone bedrock and surrounding sand ridges, as well as from igneous and other bedrocks from further upstream in the Çarşamba catchment (up to small pebbles of 5mm). These sands and gravels are typically light brown in colour, although locally they are darker brown. However, lateral variation in texture at equivalent elevations is apparent across the landscape. All locations sampled are capped by a marl layer that varies in thickness from 0.01m (core 2007/7) to 1.04m (2013/12). The marl has a clay texture in the lower parts of the complex and a silty clay texture towards the top of the complex and is predominantly light grey to white in colour.

Because of its ubiquity, the upper part of this complex was taken as the uppermost appearance of marl in the core, and its elevation varies between locations. At its deepest (core 2007/6), the upper boundary is at 6.33m below the modern ground surface, and at its shallowest (core 2007/4) it is at 1.65m. The upper surface tends to be lower between and immediately to the south of the mounds, but it also undulates in a north–south and east–west direction between cores. In the shorter cores, this complex is absent from locations 2008/8 and 9 and 2013/4.

It is of significance that within the Basal Complex there is also the presence of a laminated Dark Clay layer 1.1m below the marl, and another thin Dark Clay layer in between two marl units (see further discussion of the Dark Clay below). Two dates were obtained from the Basal Complex. One from a level of laminated Dark Clay at a depth of 3.865–3.88m produced a date of 27,617–27,011 cal BCE (2σ) on bulk organics. At a depth of 3.82–3.83m, a date of 44,666–42,555 cal BCE (2σ) on large (up to 20mm) angular shell fragments was obtained (Ayala et al. 2017: table 1).

The Lower Complex. The Lower Complex consists of silts, silty clays and clays with some reworked marl in places (fig. 2.2). The boundary with the Basal Complex is locally expressed in a variety of ways, but tends to be

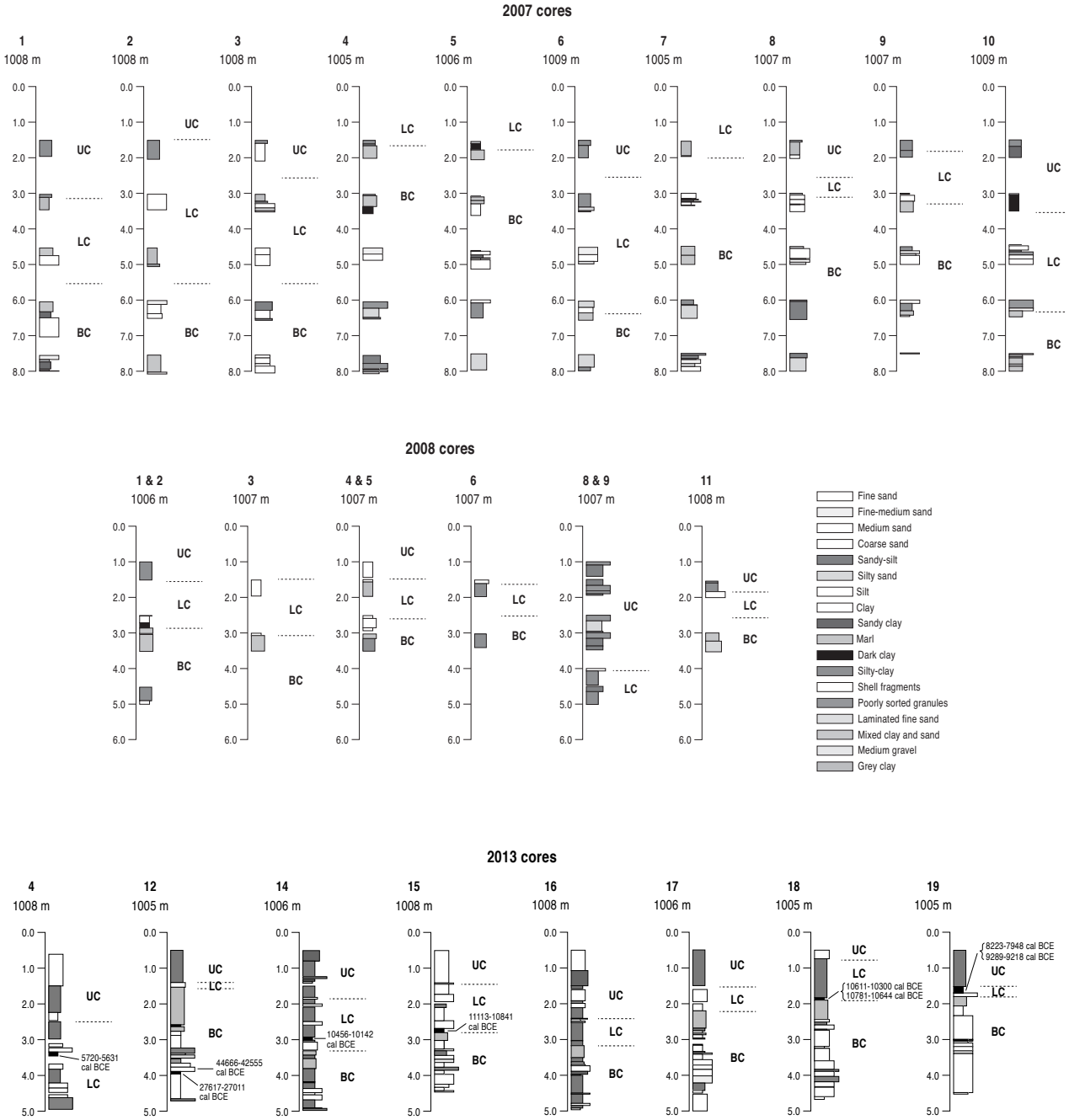

Figure 2.2. Stratigraphic sequence (2007–2013 cores) (Ayala et al. 2017: fig. 2a–c).

abrupt and smooth or occasionally wavy, suggesting erosional contacts. In a number of coring locations there is a dark grey or black clay (subsequently called Dark Clay) directly overlying the marl at the top of the Basal Complex. In some places, the boundary between the Dark Clay and the marl is irregular, suggesting intermixing due to vertic processes, as also noted by de Meester (1970: 86). Elsewhere, where the Dark Clay is absent, the Lower Complex starts with lighter coloured silts and clays, or in the case of core 2007/10, a gravel with silty matrix. In yet another core (2007/4), there is a transitionary boundary of 0.04m with the Basal Complex characterised by a mix of marl and the silt. The upper contact of the marl at the top of the Basal Complex was not observed in the other 11 cores.

The dark grey or black clay layer is also found at higher points stratigraphically in the Lower Complex in a number of cores, while being absent elsewhere. The Dark Clay varies from 1mm thick (2008/3) to between 5 and 15mm thick and is made up of coarse clay to fine silt. The dark and grey clays make up 15% (by number) of the described units in the Lower Complex from the

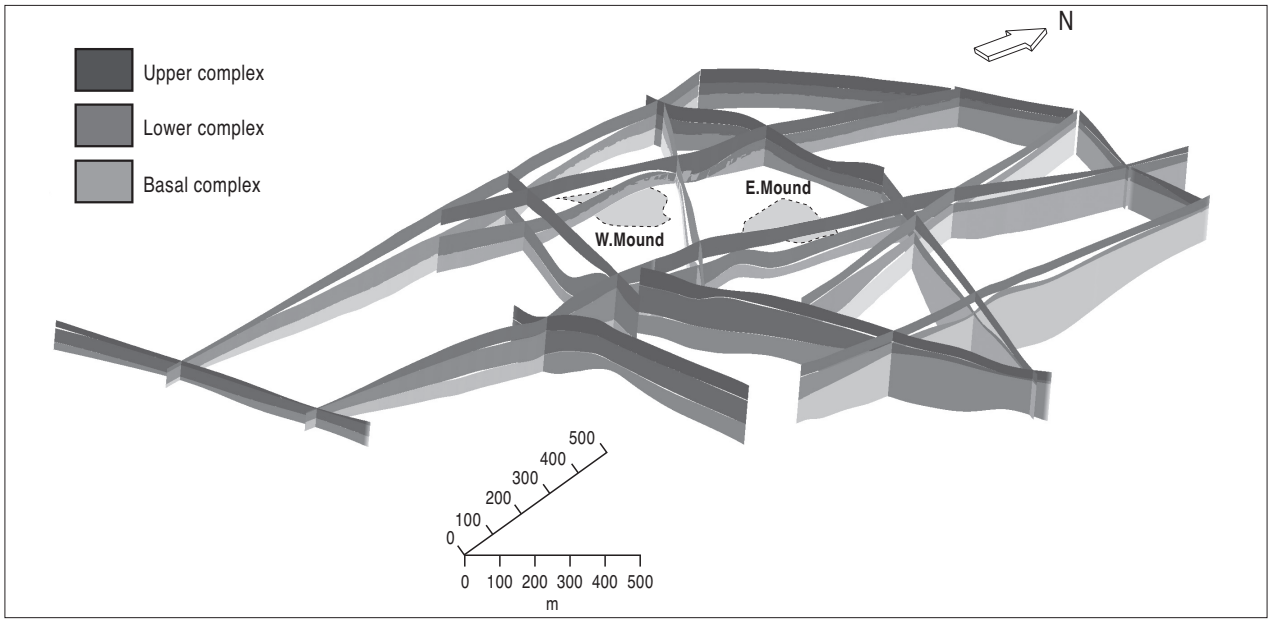

Figure 2.3. Fence diagram of the 2007–2013 cores (Ayala et al. 2017: fig. 5). The sequence at Çatalhöyük is here summarised: full sedimentological description and supporting evidence is available in Ayala et al. 2017.

2007–2013 cores. Of the remaining units in the Lower Complex, 43% are made up of silty-clays or silts, and a further 11% of clays. However, there is also a range of sands, granules and gravels, occasionally with silt matrices. Colours are predominantly from dark grey/grey to light yellowish brown.

Dates were obtained on bulk organic carbon from sediments from seven samples of the Dark Clay layer. The dates (all 2σ) range from 11,113–10,841 cal BCE to 5720–5631 cal BCE (Ayala et al. 2017: table 1).

The Upper Complex. The units of the Upper Complex are predominantly (51%) silty-clays or silts, followed by 11% of clays. Coarse sands are less frequent than in the Lower Complex, but there are still relatively frequently recorded poorly sorted granules (10%) or sandy silts (15%). There is a slight tendency for the Upper Complex sediments to be lighter than Lower Complex sediments (more dark grey/grey to light yellowish browns and fewer black to very dark greyish browns).

The transition from the Lower to Upper Complex occurs at a wide range of depths. In the majority of locations the transition sits at 1.5–2.5m below the modern surface; it can vary from 0.74 to 4.07m. Near the mounds, it is possible that colluvial deposits from the tells lead to some of this variability through the introduction of colluvial material into the alluvial sediments (e.g., Boyer 1999). This topic is currently under further investigation. However, in all locations, the Upper Complex grades up into the modern plough-soil in the upper 0.5m or so.

The Upper Complex is defined by the combination of the colour change from the grey to brown expressions of hue and the lower frequency of coarser material (sand and granule fractions). None of the measured variables (specifically, mass-specific magnetic susceptibility or organic content) were found to be significantly different from the values recorded in the Lower Complex. Further to this, it was unfortunately impossible to identify any unit with sufficiently concentrated bulk organics to provide a radiocarbon date.

Isotopic analyses comparing $\delta^{13}C$ and C/N ratios suggested that the Dark Clay layers were suggestive of standing water, riverbank soils or cutoff deposits, in slightly wetter conditions than riverbank deposits above them, or (where present) below them. Ayala et al. (2017) used these data as well as the lithostratigraphic interpretation to suggest increasingly dry conditions during the early part of the Holocene and thus during the Neolithic occupation.

Additional results from the 2015 cores

In July 2015, a further 34 cores were drilled, using the same truck-based percussion coring system as in 2013. Each core is made up of a series of three offsets in 0.5m intervals from 0.5m below the surface (as the top 0.5m is typically dry, crumbly, disturbed topsoil or track sediment which proved impossible to retain in the sample tubes) to 5.0m below the surface. The first set of offset samples is at 0.5–1.0m, 2.0–2.5m and 3.5–4.0m; the second at 1.0m–1.5m, 2.5–3.0m and 4.0–4.5m, and the third at 1.5–2.0m, 3.0–3.5m and 4.5–5.0m. This offsetting of samples is

needed to enable a continuous sequence to be recovered unaffected by disturbance from the coring process. The offsets were spaced from 5–10m apart, so some interpretation of the stratigraphic sequence is needed because of the lateral variability of the sediments. Conditions were relatively dry, so that recovery rates were often of the order of 50%, but to compensate, notes were taken of the materials in the screw threads between the sampled sections of core. These notes enabled the interpolation of the missing sections of the cores with a reasonable level of confidence.

Given that the previous samples reported in the KOPAL project and Ayala et al. (2017) are still relatively sparse away from the mounds, the purpose of the 2015 coring campaign was to broaden the landscape information away from the sites. To this end, cores were arranged in two transects of approximately 3km in length, and 0.5km to the north and south of the mounds. In this chapter, we will discuss the results from the 16 cores CH2015A–CH2015P, which form the northern transect (fig. 2.4).

The lithology of the new cores shows a similar pattern to those obtained previously. In their lower part, sequences of sands, silts and gravels pass up into one or more levels of marl (except for core CH2015F, where no marl was present in the 5m sampled). The sands and gravels are subrounded and subangular, and have mixed lithologies and local presence of shell fragments. The topmost level of marl varies from 0.10 to 0.46m thick. There is a darker clay within the marl sequence in core CH2015O, in patches at depths of 3.88–3.68m below the surface (the upper marl surface is at 3.07m below the surface in this core).

In the central part of the transect, the marl is followed by darker clays (cores CH2015G and CH2015I–CH2015K). Elsewhere, there is a darker level after a series of silty deposits in both CH2015H and CH2015L, or lighter silty and clay deposits lie immediately above the marl. The only other core with a Dark Clay immediately above the marl is CH2015P, which is at a relatively low elevation. Silts, clays and sands make up the following deposits, and they are typically dark grey/grey to light yellowish brown. The upper part of the sequence is made up of dark grey/grey to light yellowish brown silts and clays, with occasional sands including coarse sands.

As noted above, CH2015F has no marl. It passes straight from yellowish brown sands and silts to darker grey and brown sands. We interpret this sequence as representing a Holocene channel that has incised through the upper marl into the channel deposits in the later Pleistocene sequence. The presence of gravels, and medium and coarse sands at some points in adjacent cores CH2015E and CH2015G, as well as a crop mark visible on imagery suggests this was a relatively wide, meandering channel with a width of 60–80m. Similar deposits were sampled in a drainage ditch section about 100m to the south in 2017 with the aim of obtaining OSL dates (results pending).

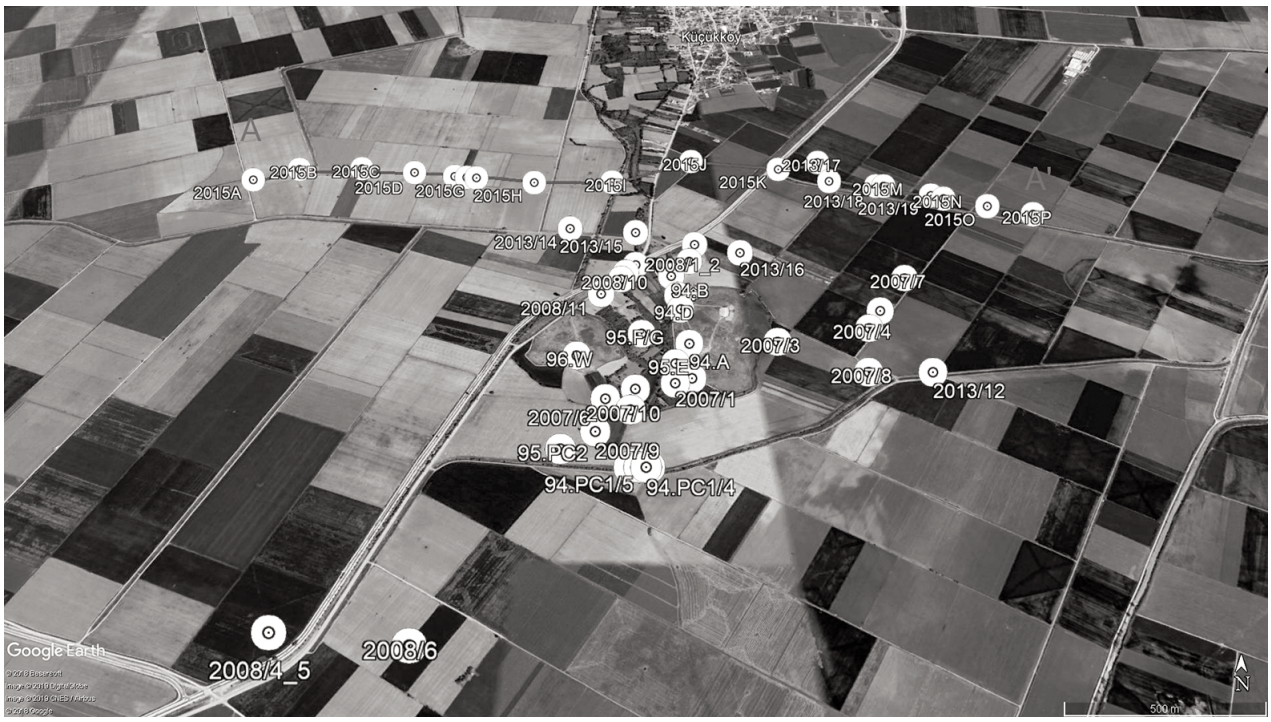

Figure 2.4. Map of coring locations in relation to the two tells at the site. The east/west transect to the north (at the top of the image) shows the location of the section A-A' used in the interpretation of the lithology and stratigraphy of the northern transect sampled in 2015 (figs 2.5 and 2.6).

Figure 2.5. Lithological logs of the cores CH2015A–CH2015P along section A-A' (see fig. 2.4). Elevations of the tops of the cores are estimated from the SRTM DTM.

Stratigraphic interpretation of the cores from 2015 (fig. 2.5) is based on the same sequence as described above. A Basal Complex is present in all the cores and interpreted as being the channels topped by the marl of Palaeolake Konya (except for CH2015F, where the uppermost marl is interpreted as having been eroded by the later channel). The Basal Complex recovered varies from 0.23m to 2.06m in thickness. The elevation of the upper surface is irregular and varies by up to approximately 5m. The Lower Complex contains sediments again suggestive of an anastomosing channel system, and the lower palaeoelevations from CH2015C to CH2015J and CH2015L and CH2015M would have provided accommodation space for this channel system to accumulate. At CH2015E–G, the sediment colour suggests incision into the Pleistocene surface in the earlier part of the Holocene, which may be compatible with the dates on the palaeochannel PC94/1 (Boyer 1999; Boyer et al. 2006), although this hypothesis remains to be confirmed. Sediment thicknesses from CH2015C and CH2015D suggest a later channel incision, but this feature does not seem to correspond to any crop marks in imagery we have seen. The Upper Complex again passes up into the plough-soil and is generally thinner at the extremities of the transect, in places as thin as 0.94m, but locally just over 4m thick. Figure 2.7 is an updated fence diagram showing the refinement of the understanding of the palaeosurfaces at different times.

We are in the process of carrying out detailed XRF analyses of the cores in order to improve the interpretation of the local depositional conditions. Analysis has been carried out using a GeoTEK Multi-sensor core-scanner system at Durham University. Figure 2.8 shows a section from core CH2015K, chosen because it shows a clear transition from the uppermost marl at 1.87m below the surface through a gradational boundary with a Dark Clay layer (10YR3/2 and locally 10YR2/1 with marl and rolled clay fragments to 3mm diameter). The Dark Clay is 0.13m thick and has a gradational boundary with a silt deposit (10YR5/2 with numerous white and orange inclusions), which continues to the top of the illustrated section. The GeoTEK also allows measurement of magnetic susceptibility, which has low values in the marl (average 6.0×10^{-5}), increasing through the Dark Clay (average 2.7×10^{-4}) and through most of the silt deposit (average 4.7×10^{-4}; lower values in the topmost part of the core are likely due to sampling errors from irregularities in the core). The Incoherent/Coherent (Inc/Coh) scattering ratio has been found to be a useful proxy for organic matter content (Croudace, Rothwell 2015). Although the values are slightly higher in the Dark Clay, there is not a large difference from either the marl or the overlying silt. This pattern is consistent with the small difference in organic matter content in the Dark Clay, as reported previously by Boyer (1999), Ayala et al. (2017) and Doherty (2017). Hierarchical clustering (calculated using the rioja package in R: Juggins 2019) on these signals as well as the elemental data shows that the chemistry of the marl is distinct from the Dark Clay and silt layers, and as might be expected, most notably in the Ca content. It also suggests that there is a more gradational change from the Dark Clay into the silt than is apparent to the naked eye.

As well as looking at the elemental data from the XRF analysis, it is often useful to look at ratios of certain elements to make palaeoenvironmental analyses (Davies et al. 2015). The Inc/Coh ratio values are significantly different in the three layers (ANOVA: $p=9.87 \times 10^{-5}$; post-hoc comparisons show the values for the Dark Clay are higher than either the marl below or the silt above). This pattern is consistent with that found by Ayala et al. (2017) and in earlier studies (Boyer, 1999), although the absolute

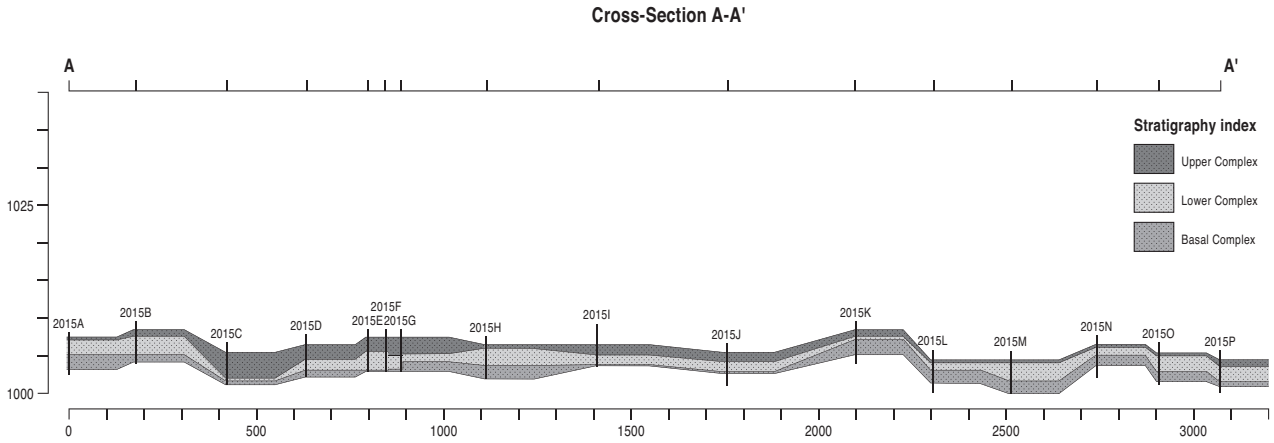

Figure 2.6. Sedimentological correlation of the cores CH2015A–CH2015P along section A-A' (see fig. 2.4). Elevations of the tops of the cores are estimated from the SRTM DTM.

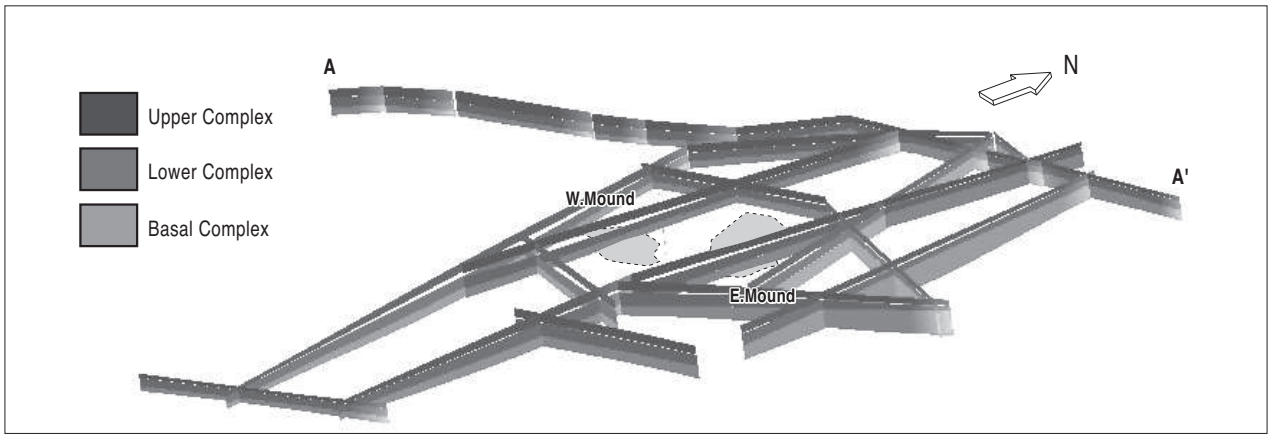

Figure 2.7. New fence diagram showing the impact of the new cores CH2015A-A' (compare with fig. 2.3) in the landscape interpretation.

differences – which have yet to be calibrated for this core – are only of the order of 2%. The K/Ti ratio suggests that catchment pedogenic processes are dominated by physical weathering in the marl, with a shift to progressively more chemical weathering in the dark silt. The values are significantly different according to the lithology (ANOVA: $p=3.74 \times 10^{-15}$; post-hoc comparisons suggest the marl is different from the Dark Clay, but the latter is indistinguishable statistically from the silt). The Rb/Sr ratio suggests that chemical weathering is dominant in the Dark Clay and silt (ANOVA: $p=2.47 \times 10^{-6}$; post-hoc comparisons suggest that the difference is again between the marl and the upper deposits), and the curve should be broadly inverse to that of K/Ti. These patterns are consistent with the shift from physical weathering processes in the colder conditions of the upper Pleistocene to the warmer and wetter conditions of the Holocene producing more chemical weathering and soil formation (Wainwright, 2009). De Ridder (1965) also notes different sources of heavy minerals from the May and Çarşamba, and it is possible that changes in source areas may also cause the ratios to change. This is the subject of ongoing investigations. It has been suggested that the Fe/Mn ratio relates to redoximorphic conditions in sediments or the soils contributing to them. The values are significantly different from each other (ANOVA: $p=7.68 \times 10^{-10}$), with the Dark Clay layer being significantly higher than either the marl or the overlying silt. Thus, the Dark Clay probably had higher redox potential, suggesting that it was more consistently in contact with the atmosphere. This interpretation is consistent with that of Doherty (2017) that the Dark Clays may be remnants of vertisols, so intermittently dry, which is also consistent with the isotopic results presented by Ayala et al. (2017) that suggested at least some periods of standing water, and the relatively low differences in the organic matter contents. Finally, the ln (Zr/Ti) ratio is considered to be a proxy for particle size. There is an increase through the core, which is significantly different according to the lithology (ANOVA: $p=1.03 \times 10^{-14}$), although the Dark Clay is not significantly different from the marl according to the post-hoc comparisons.

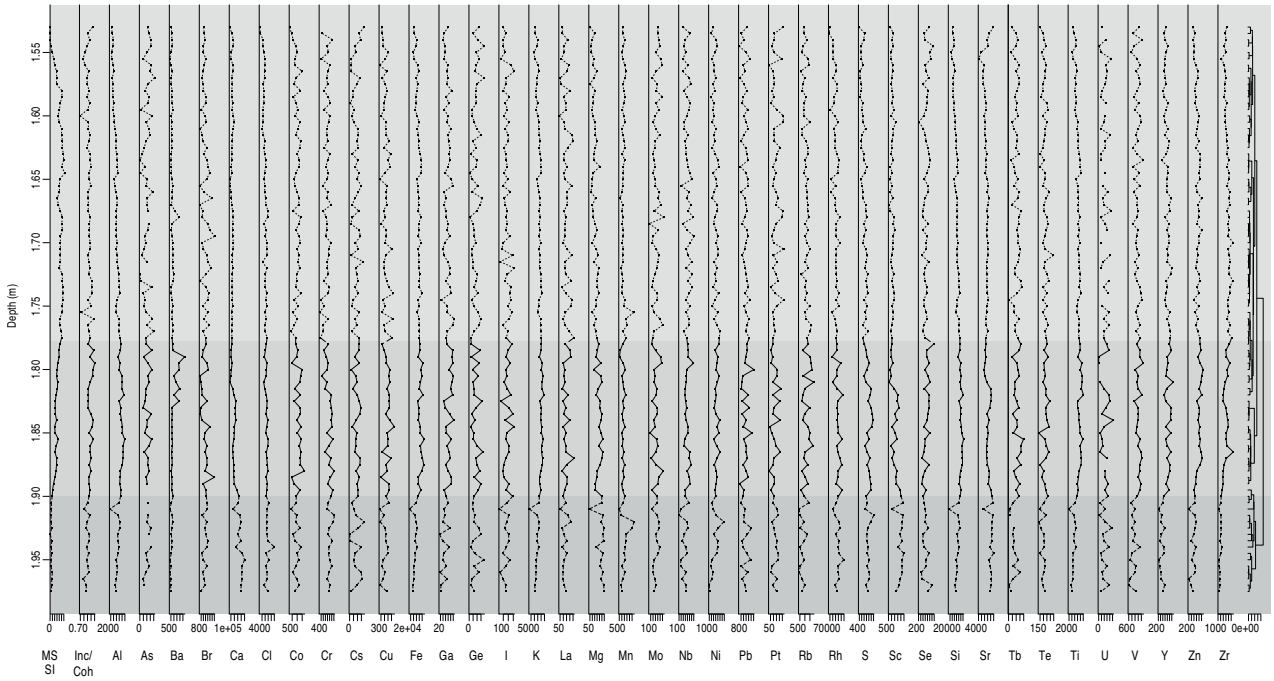

Figure 2.8. Example of Micro-XRF analysis of core CH2015K. First column on the left, MS SI = magnetic susceptibility (10^{-5} SI), while the second column, Inc/Coh ratio provides a proxy for organic matter content (Croudace, Rothwell 2015). Remaining panels are area estimates for the different elements analysed, showing the relative contents of each. The dendrogram on the right is based on hierarchical clustering (calculated using the rioja package in R: Juggins 2019) and shows that the marl is significantly different from either the Dark Clay or the Lower Complex silt. The two latter deposits are more closely related to each other. The background is shaded according to lithology: the lower dark grey is the marl, the middle medium grey is the Dark Clay and the upper light grey is the Lower Complex silt.

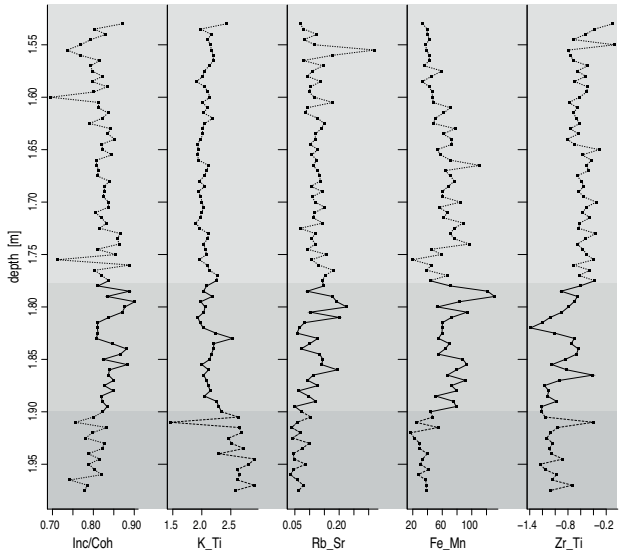

Figure 2.9. Series of ratios of micro-XRF analyses used in previous studies for palaeoenvironmental interpretation. The background is shaded according to lithology: the lower dark grey is the marl, the middle medium grey is the Dark Clay and the upper light grey is the Lower Complex silt.

Summary of palaeolandscape reconstruction

The 2015 data strengthen the interpretations of Ayala et al. (2017) and allow us to add nuances to the four-phase reconstruction (fig. 2.10). After the retreat of Palaeolake Konya from the site in the late Pleistocene, Phase 1 consists of a single-thread and possibly ephemeral channel (with a relatively low flow: see below) that made its way through a landscape dominated by local wind and water erosion. The topography probably resembled a marl 'badland' with a rolling topography varying by 7m or so. The 2015 transect demonstrates that this surface also had larger-scale low points, allowing the subsequent channels to occupy a belt of several hundred metres in width. In Phase 2, these channels were consistent with a humid anabranching system (fig. 2.10), with localised areas of wetter conditions where low points persisted, or where channel cutoffs occurred. Evidence from the Dark Clay layers puts this phase as being from 11,113–10,841 cal BCE to 8223–7948 cal BCE (2σ), and thus it predates settlement of the East Mound. Although the rolling topography starts to infill in Phase 3, there are still relatively wide areas available for the anastomosing channel belt to occupy, as it transforms into

a more dryland anabranching system. Lewis et al. (2017) studied *Unio* fossil shells from the site (spanning the occupation period ca 7200–6050 cal BCE) and suggested that the bivalves likely lived in small lakes/wetlands around the site before being gathered and taken to Çatalhöyük. Wet-dry seasonal cycles occur in the shell oxygen isotope ($\delta^{18}O$) profiles with low winter values reflecting winter precipitation and high $\delta^{18}O$ in the summer resulting from evaporation. The most striking trend in the $\delta^{18}O$ data is the drop in maximum summer $\delta^{18}O$ ca 6350 years BCE, interpreted as lower summer evaporation and hence a reduction in seasonality. The shift in seasonal climate could be due to solar-forced climate change beginning ca 6650 cal BCE (see also fig. 2.11). Although these data have previously been used to support the fission-fusion farming hypothesis in that they show wet winter/early spring conditions during the Early Holocene which could have caused flooding, they also support the present reconstruction of seasonally flooding anastomosing channels. Again, localised pockets of wetness persist into the Chalcolithic in this setting, with a single date on a Dark Clay at 5720–5631 cal BCE (2σ). Therefore, our fourth phase probably starts during or just after the Chalcolithic, with a shift to a larger, probably single-thread channel (with a significantly higher flow: see below), which probably persisted to the present period until the Çarşamba was channelised.

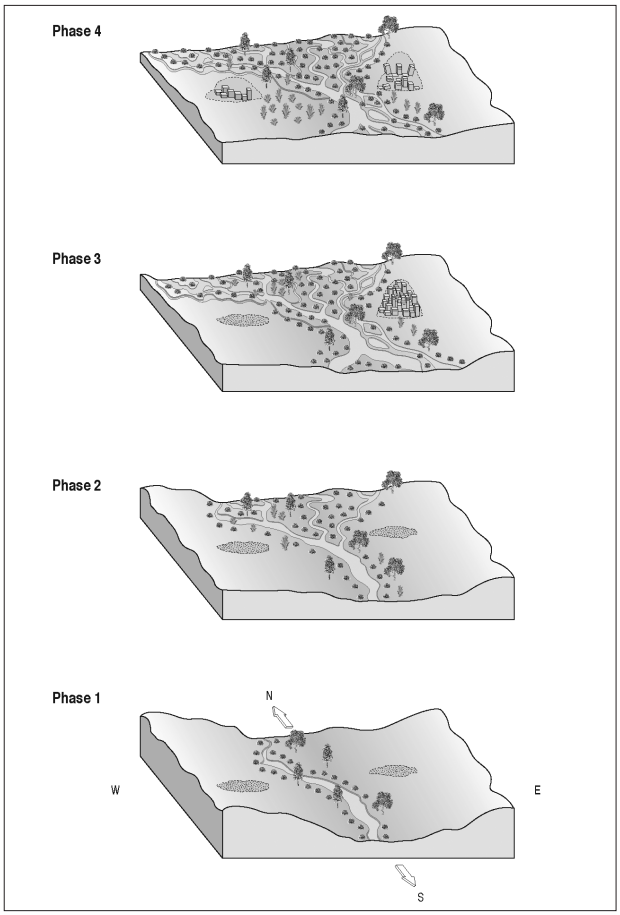

Figure 2.10. Palaeohydrological reconstruction of Ayala et al. (2017: fig. 9) with superimposed interpretation of vegetation patterns based on the discussion in the text.

Pollen and palaeoenvironmental proxies

Vegetation of the Konya Plain during the occupation of Çatalhöyük

Since the palaeoenvironmental review of Çatalhöyük (Charles et al. 2014), more information has emerged regarding the climate and vegetation of the Central Anatolian Plateau (Roberts et al. 2016; Eastwood 2018; Woodbridge et al. 2019). This information helps to refine our previous model for the nature of vegetation and land use around Çatalhöyük during its occupation.

Charles et al. (2014) suggest that site occupation of Çatalhöyük (7100–6050 cal BCE = 9100–8000 cal BP) (Bayliss et al. 2015; Marciniak et al. 2015a; Orton et al. 2018) coincided with a period of relatively warm, wet conditions in comparison to the cold, dry Younger Dryas period. The vegetation reconstructed from pollen cores (Lake Nar, Eski Acıgöl and Akgöl) was relatively moist forest/grass steppe characterised by high levels of Oak (*Quercus* sp.), and grass (Poaceae) pollen. In their subsequent work, Roberts et al. (2016) compare the results from two lakes (Lake Nar and Eski Acıgöl). They include oxygen-isotope data that provide the basis for subsequent discussion. In addition, data from the cores allows inference of vegetation (pollen), lake levels (diatoms) and river influxes (calcite). These additions provide more evidence for broad vegetation trends for our reconstruction (table 2.1), though it must be noted that the period of site occupation is still only represented by fewer than ten samples.

Based on a set of hydroclimate proxies from Nar Lake, Roberts et al. (2016) infer wet and dry phases for the period of occupation at Çatalhöyük (table 2.1). These indicate that Çatalhöyük was initially settled towards the end of a relatively dry period (7550–7150 BCE). The subsequent 500 years are shown as an intermediate period of moisture before a ca 500-year period of relatively dry conditions terminating ca 6250 cal BCE. The vegetation of the region prior to occupation (8750–7250 cal BCE) is characterised as that of oak-pistacia woodland, typical of fairly dry conditions. The early occupation of Çatalhöyük in contrast coincides with the development of oak steppe-parkland characteristic of wetter conditions.

Woodbridge et al. (2015) use the pollen records from a series of sites across Southern Anatolia to create a chronological sequence of the predominant inferred vegetation present in the region. Eski Acıgöl, the only site on the Anatolian Plateau for which there is a continuous record for the period of Çatalhöyük's

occupation, shows a remarkable level of vegetation continuity through the Early to Late periods, a period made up of parkland/grassland. This 'vegetation cluster' comprises a relatively open landscape characteristic of relatively moist conditions, dominated by grasses, members of the Asteraceae family and open oak woodland (Woodbridge et al. 2018). It changes to a more arid vegetation made up of sclerophyllous parkland in the Final period. Similar changes to more arid vegetation are also seen at Akgöl (on the plateau) and Beyşehir to the southwest, though nearby Gölhisar shows no change.

Moving our attention to a more local picture of vegetation on the Konya Plain, Kabukcu (2017) provides a detailed view based on wood charcoal evidence from Çatalhöyük and two other sites (Boncuklu, Can Hasan III). Evidence from the latter shows high levels of willow (Salicaceae) and low levels of oak in the period prior to occupation at Çatalhöyük. The Early period of Çatalhöyük continues this picture before there is a substantial increase in oak values in Levels South G-H that coincides with the rise in oak pollen values in the Eski Acıgöl and (to a lesser extent) the Nar cores. The high oak charcoal values continue through to Level South P when juniper (*Juniperus*) values become dominant, along with almond (*Amygdalus*) and pistachio (*Pistacia*), potentially indicating increasing aridity. Evidence for river conditions based on riparian woodland taxa shows an abundance of willow and the elm family (Ulmaceae) in the Early period that is replaced by ash (*Fraxinus*) in the later period that could indicate a change in river hydrology consistent with the other evidence presented in this chapter.

Isotopic evidence

Roffet-Salque et al. (2018) used δ^2H analysis from lipids on pottery in well-dated contexts at Çatalhöyük (fig. 2.11a) to suggest that there was a climate change that correlated with the 8.2kya event recorded in Greenland ice cores (fig. 2.11b) and elsewhere. Following our critique (Wainwright, Ayala 2019), Roffet et al. (2019) agreed that the fluctuation in their data is not statistically significant and that the sequence shows a high degree of variability. This observation is consistent with the idea that the local climate was dominated then as now by high degrees of interannual variability. Figure 2.11c shows that the ~8.2kya excursion at Nar that Roffet-Salque et al. (2018) used to suggest there was regional evidence for was actually part of a longer series of oscillations that started much earlier and thus cannot be correlated with the Greenland event. Wainwright and Ayala (2019) also used the proxy data from Jones et al. (2005) to suggest that the maximum summer temperature was a reasonable proxy for the Nar isotope data, and that it varied little over the period in question (fig. 2.11d). Roffet-Salque et al. (2018) followed Dean et al. (2016) in stating that the proxy is more related to water availability (precipitation/evaporation), but if there is no evidence that precipitation varied other than on an interannual basis (and the proxy estimates are smoothed to minimise this effect), then these two interpretations are not incompatible, as Dean et al. (2016) calculated evaporation from temperature data. In figure 2.11e, we address the effectiveness of the Nar proxy (in our case, for temperature) for Çatalhöyük, using the relation between the CRU TS4.01 reconstructed JAS maximum temperature 1901–2016 (Harris et al. 2014) for the 0.5° grid cells containing Nar and Çatalhöyük. This relation is highly significant (r^2=0.943, $p < 2.2 \times 10^{-16}$), but because these data are both interpolations from other sites, the strength of the relation is likely to be overestimated. Thus, figure 2.11f has instrumental data for JAS mean temperature from Niğde and Konya for the period 1951–2001, which is also highly significant (r^2=0.428 and $p=1.919 \times 10^{-7}$).

Reconstructing the palaeohydrology of the Çatalhöyük landscape

In Ayala et al. (2017), we challenged the interpretation of Roberts and Rosen (2009: 397) that the Neolithic environment was of 'backswamp basins gradually infilled' by spring floodwaters for two reasons: first, the more waterlogged conditions suggested by the Dark Clay layers are earlier than occupation (except for a localised outlier that dates to the Chalcolithic); and second, the anastomosing channel system is not compatible with the interpretation of a backswamp (see further discussions on the latter point by Charles et al. 2014 and Doherty 2017). Here, we address further issues with the spring floodwater model of Roberts and Rosen (2009) through a discussion of the data used to build their model and the modelling method that was subsequently used to estimate flooding regime at the time. The data upon which they build their hydrological interpretation come from Bozkir because the extensive channelisation schemes in the late 19th and early 20th centuries (especially the Beyşehir-Çarşamba Canal) and the dam at Apa significantly altered the flows in the lower part of the Çarşamba, so that modern instrumental records are not useful for interpreting the possible Neolithic flow regime. It should be noted that Bozkir is a long way upstream (32° 12' 34" N, 37° 10' 24" E), at an elevation of 1156m with a catchment area of only 206km^2, compared to an estimated 2,079km^2 for the Neolithic Çarşamba just downstream of Çumra (estimated using ArcMap hydrological analysis on the SRTM 30m DTM by adding an artificial blockage to the catchment just upstream of

<table>
<tr><th>Çatal Occupation [a]</th><th>Dates cal BCE [b]</th><th>climate [c]</th><th>Lake Nar [d]</th><th>Eski Acıgöl [e]</th><th>Akgöl [e]</th><th>Beyşehir [e]</th><th>Gölhisar [e]</th></tr>
<tr><td>POST-</td><td></td><td></td><td></td><td></td><td></td><td></td><td></td></tr>
<tr><td>Final 6300-5950 BCE</td><td>6200-5300</td><td>wetter</td><td rowspan="5">oak steppe-parkland [grasses & artemisia] (NG-4)</td><td rowspan="2">dry park</td><td>dry park</td><td rowspan="2">dry park</td><td>park/ grass</td></tr>
<tr><td rowspan="3">6700-6200</td><td rowspan="3">drier</td><td>steppe park</td><td rowspan="4">pine wood</td></tr>
<tr><td>Late 6500-6300 BCE</td><td rowspan="3">park/ grass</td><td rowspan="2">pine steppe</td><td rowspan="3">pine wood</td></tr>
<tr><td>Middle 6700-6500 BCE</td></tr>
<tr><td>Early 7100-6700 BCE</td><td>7200-6700</td><td>intermediate</td><td>[no data]</td><td>dry park</td></tr>
<tr><td rowspan="2">PRE-</td><td>7550-7200</td><td>drier</td><td rowspan="2">oak-pistacia (NG-3)</td><td rowspan="2">park/ grass</td><td rowspan="2">steppe park</td><td></td><td></td></tr>
<tr><td><7550</td><td>wetter</td><td>pine wood</td><td>deciduous oak parkland</td></tr>
</table>

Table 2.1. Palaeoenvironmental reconstruction of conditions on the Anatolian Plateau and surrounding region during the occupation of Çatalhöyük: (a) occupation periods and their chronology; (b) dates – BCE calibrated for palaeoenvironmental indicators; (c) climate as defined by Roberts et al. (2016), shading showing their interpretation of relative dryness (but cf. figure 2.11); (d) Lake Nar data summarised from Roberts et al. (2016); (e) pollen records summarised by Woodbridge et al. (2019). Park/grass = parkland/grassland; dry park = sclerophyllous parkland; steppe park = steppe parkland.

where the Beyşehir-Çarşamba Canal joins the main stem of the Çarşamba River). Thus, the catchment area feeding the channel system at Çatalhöyük is an order of magnitude larger than that producing the flow at Bozkir. As noted by Roberts and Rosen (2009: 396), 'the Taurus Mountain region above Bozkir receives high precipitation, much of it as snowfall, whose melting gives rise to the main annual river flood peak in March and April'. However, much of the rest of the catchment is at lower elevation and receives less precipitation as snowfall. Precipitation is also more evenly spread through the year. For example, at Çumra, the 1961–1990 monthly means are very similar from October to May, between 31 and 45mm, dropping to 19mm in June and 0mm between July and September. Although some of this precipitation is in the form of snowfall, more of it is as rain, so that runoff and river flow may well have been more evenly spread through the year in the lower Çarşamba.

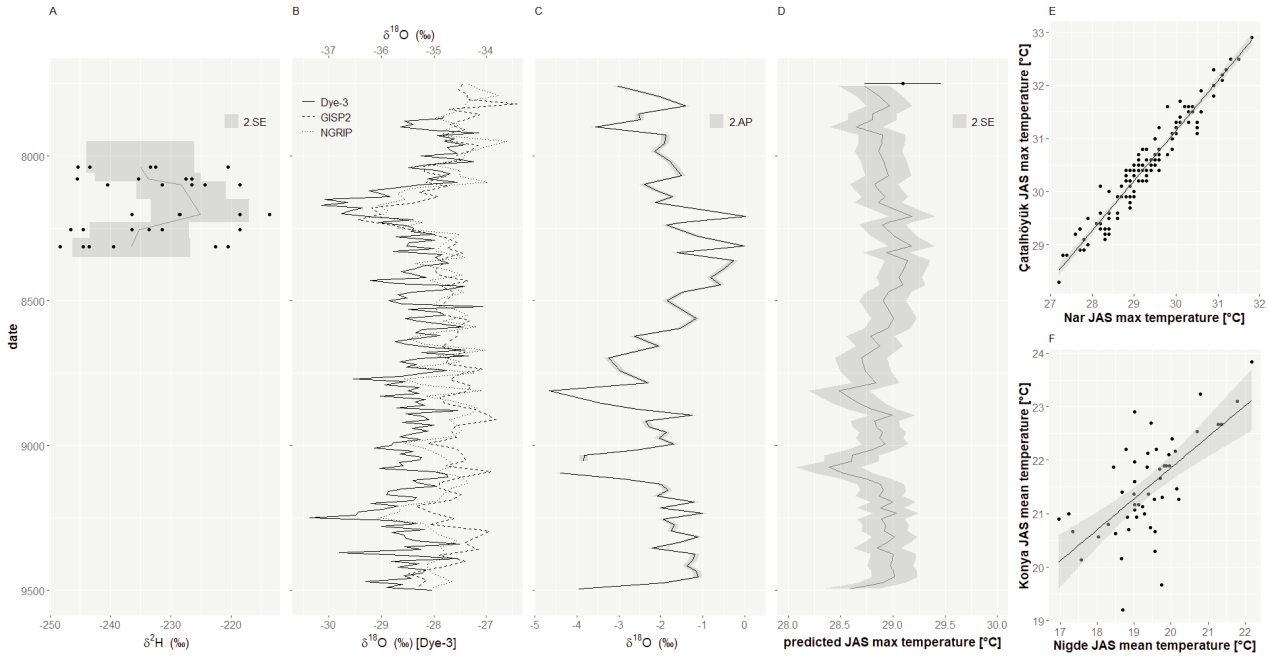

Figure 2.11. Comparison of the $\delta^2H_{18:0}$ proxy of Roffet-Salque et al. (2018) with global and regional climate records. This plot uses a window from 9000 to 7800 calibrated B.P. to place the proxy data in a longer-term context consistent with the discussion in the text here: (a) replots the data of figure 1D in Roffet-Salque et al. (2018) using shading to show the 2-SE variation of data around the mean (solid line); original data points are plotted at the midpoint of the archaeological phase, but shading is shown vertically to demonstrate the full uncertainty of the Bayesian estimates of these phases. There is clear overlap between the phases, and variability is more important than mean values; (b) water $\delta^{18}O$ values of three Greenland ice cores (Stuiver et al. 1995; NGRIP Dating Group 2006; Vinther et al. 2006; Rasmussen et al. 2007) used to demonstrate the onset and duration of the 8.2kya event; (c) $\delta^{18}O$ record from the sediments in Nar Lake (Jones et al. 2005), ~150 km from Çatalhöyük, which provides the best available regional information for climate proxies. Shaded area shows 2× analytical precision (AP) of the measurements; (d) estimate of summer maximum temperature for Nar Lake, based on the proxy derived by Jones et al. (2005) from modern climate measurements. The shaded area is 2 SEs, using a RMS combination of the uncertainties from the measurement analytical precision and the SE from the proxy model. The point and error bar at the top of the plot show the mean and 2-SE range for the 1961–1990 climatic observations; (e): relation between CRU TS4.01 (Harris et al. 2014) reconstructed JAS maximum temperature 1901–2016, $r^2=0.943$, $p < 2.2 \times 10^{-16}$; (f): instrumental data for JAS mean temperature from Niğde and Konya 1951–2001, $r^2=0.428$, $p=1.919 \times 10^{-7}$ (based on Wainwright, Ayala 2018).

A common, simple method for estimating flows progressively downstream in an ungauged catchment is to fit a power-law model of the form $Q = a A^b$, where Q is the discharge (in $m^3 s^{-1}$), A is the catchment area (in km^2) and a and b are empirical coefficients. Based on monthly average data from the Turkish Hydrological Service (DSI: http://www.dsi.gov.tr), an attempt was made to extrapolate flows using the available sites upstream of the modern diversions in order to estimate the pre-modern flow accumulation. Measurements are available from the stations at Sorkun (32° 8' 58" N, 37° 9' 56" E), Bozkir and Pinarcik (32° 16' 49" N, 37° 15' 47" E), which have catchment areas of 84.0km^2, 205.6km^2 and 343km^2, respectively. However, for all months except February, the mean monthly flow at Pinarcik is lower than Bozkir, and it is not possible to fit a significant model using the catchment area. The implication of this observation is that the runoff coefficient (the proportion of precipitation that is converted into flow) decreases in the lower part of the catchment and/or there are significant transmission losses (infiltration from the channel into the channel bed). Both are common characteristics of dryland channels, as a result of spatial variability in vegetation and soils, temporal variability of rainfall intensity during thunderstorms, and unsaturated subsurface conditions between storm events (Parsons et al. 1999; Wainwright, Parsons 2002; Yair, Kossovsky 2002; Wainwright, Bracken 2011), and some parts of the Çarşamba catchment are also karstic.

Given these limitations of the data, a simple way to estimate likely mean flows for the lower Çarşamba is to use estimates from the flow yield (discharge per unit area

of catchment) at each of the known stations, and then multiply by the catchment area at the point of interest (2,079km^2 in this case). The estimated values are as follows for the 'spring flood' period (table 2.2).

Because of the downstream losses, all of these estimates are likely to be overestimates, with those based on the most downstream station (Pinarcik) integrating more of these effects and thus likely to be more reasonable. Based on modern data, the highest mean flows are about 2 to 2.5× these values, although it should be remembered that these values would still be for monthly averages, not peak flood flows. In comparison, it is possible to estimate the bankfull conveyance (discharge that can be carried before flooding occurs) of the two palaeochannels observed near to Çatalhöyük using the Manning equation. Assuming there is no truncation of the channel profiles in Boyer (1999), Chalcolithic palaeochannel 95/PC2 has an area of 38.2m^2, an estimated wetted perimeter of 34.9m, and thus a hydraulic radius of 1.1m. If the former channel slope was subparallel to the modern surface (probably an underestimate), and using Manning's n values of 0.025 to 0.033, characteristic of a channel that is 'clean, straight, full stage, [with] no rifts or deep pools' (Chow 1959), the bankfull conveyance would have been between 62 and 82m^3 s^{-1}. Palaeochannel 94/PC1 is much larger, with an area of 126.2m^2, wetted perimeter of 54.4m and hydraulic radius of 2.3m, so that with the same assumptions, its bankfull conveyance would be between 338 and 446m^3 s^{-1}. Bankfull discharges of channels tend to adjust to the mean annual flood (Dury 1973). If both 94/PC1 and 95/PC2 were single-thread channels (as the Çarşamba was known to be historically), then these estimates would imply that 94/PC1 was formed in a much drier period than 95/PC2, which is consistent with other climatic observations from the late Pleistocene and Chalcolithic, respectively, when these channels were formed. Palaeochannel 95/PC2 would easily have been able to convey the peak mean flows estimated above without flooding. Although it must be remembered that the above estimates do not account for extreme flood flows, the data suggest that the Chalcolithic channel was adjusted to higher flows than at present.

Estimate using station	*Estimated mean monthly flow m^3 s^{-1}*			
	Feb	*Mar*	*Apr*	*May*
Sorkun	61.1	106.5	159.5	116.2
Bozkır	4.3	85.7	108.8	63.9
Pınarcık	23.7	45.1	53.7	2.8

Table 2.2. Estimated mean monthly flows for the lower River Çarşamba using three measuring stations in the upper reaches of the River Çarşamba during the months of February–May based on data from Devlet Su Işleri (http://www.dsi.gov.tr/).

However, Ayala et al. (2017) demonstrated that the earlier Holocene channels of the Çarşamba were most likely to be multi-thread, anastomosing channels. The problem with these channels is that it is impossible to estimate the past channel dimensions directly from the stratigraphic record (Nanson, Knighton 1996), even if there were available exposures locally. Furthermore, there have been very few studies of the flooding characteristics of this style of channel, not least because of the difficulties of making measurements. Entwistle et al. (2018) used a modelling approach to look at contrasting single-thread and anastomosing reaches of the River Wear to show that the styles of flooding were very different in the different reaches. Although care must be taken in extrapolating from an upland, gravel-bed channel in the UK, their results suggest that the anastomosing system will typically flood more frequently, but it also has the effect of spreading out the flow more broadly. As a consequence, the anastomosing system has lower shear stresses, leading to more stable surfaces, that is, less likely to erode and more likely to have sediment deposition. Sediment deposition would have led to there being progressively higher capacity for subsurface water storage, and thus progressively less extreme floods through time, and potentially the increasingly 'dry' anastomosing channel types in the record. Flooding may have been extensive but restricted to the locally lower points in the landscape, which suggests it could have been only a kilometre or so across, thus leaving extensive, unflooded areas close to the site that would have been available for cultivation. As noted above, the inherent heterogeneity of dryland environments is key to understanding the complexity and ephemerality of the environment, which would have influenced the choices made by the occupants of Çatalhöyük over time.

Conclusions

The palaeoenvironmental record of the Çarşamba River plain provides key information to further our understanding of the entangled nature of the relationship that occupants of Çatalhöyük had with their landscape. Fundamental questions surrounding agricultural production and organisation at the site require high-resolution palaeoenvironmental evidence which can support robust environmental models and interpretations of behaviour. The intensive coring programme has enhanced the previous landscape models, derived from a limited number of data points (Boyer 1999; Boyer et al. 2006). We have redefined the stratigraphical record and

hence re-propose the alluvial development of the area into four phases (Ayala et al. 2017). During the early Holocene, when the site was occupied, the immediate environment was dominated by a multi-thread anastomosing channel instead of a single meandering one. The analysis of the most recent cores (2015) and modelling of the palaeohydrological evidence suggests that flooding in the area would have not created the backswamp once imagined (Roberts, Rosen 2009) but would instead have left areas of high ground which would have been suitable for agriculture. This more nuanced reconstruction of the Çarşamba River plain will enable us to write more accurate and meaningful interpretations of the relationships, and long-term interdependencies, that the Neolithic inhabitants had with their environment.

Returning to previous interpretations of entangled behaviour, whilst there is undoubtedly evidence of human manipulation of the floodplain, for example, the pits near the tell, the interpretation of their impact on the alluvial environment and the watertable requires a higher resolution model of the alluvial landscape. Our work has demonstrated how powerful this level of accuracy can be to test traditional models of climate change (Wainwright, Ayala 2019) and to reinterpret past land use (Roberts, Rosen 2009). The reinterpretation of the sedimentary sequence coupled with the modelling of the channel flow has supported our reconstruction of the development of the dryland anastomosing channel system and hence the increasing potential for dryland agriculture in the immediate vicinity of the tells throughout the Neolithic and Chalcolithic, which supports evidence for demographic growth of the settlement and the development of garden-type agriculture throughout the Neolithic (Bogaard 2005).

Although the localised flooding in lower-lying areas occurred throughout the period of occupation, the anastomosing system created a range of ecological niches that could have supported a diverse range of cropping strategies in the areas immediately surrounding the site. Archaeobotanical evidence suggesting a preference for more drought-tolerant barley species being selected at the tells (Bogaard et al. 2017) is consistent with this observation. The entangled nature of life in the alluvial environment thus requires us to consider how environmental niches that support resilience in the Neolithic settlement of Çatalhöyük are created through the agency of the alluvial landscape, bringing water and sediment to the local landscape. This agency is modified by the use of sediment and water for cultivation, creating a landscape that is accreting vertically and helping to enhance the dryness of the landscape, buffering the fluctuations in climate. As the tell built up, it provided a further sediment source, and the coupling of colluvial and alluvial processes created a yet further, more complex landscape. The agency of the mound produces conditions where the channel belt tends to be diverted away from the settlement, and thus locally more conducive conditions for habitation and sustainable agriculture.

Future work is needed to refine these entangled models of human-landscape interactions, because the complexity of dryland environments requires evidence at as high a resolution as possible. As well as further sedimentological analyses immediately surrounding the site (for example, looking at colluvial-alluvial interactions) and in the immediate vicinity (for example, to look at changing patterns of the channel belt through time), a larger landscape context is needed to look at the source and sinks of sediment, and thus patterns of land available for cultivation and other uses. Future palaeohydrological modelling will evaluate patterns of seasonality in more detail, as well as the impacts of longer-term climate variability. Scales of variability – in both space and time – are fundamental to the understanding of this landscape.

Acknowledgements

The authors wish to thank Ian Hodder for supporting sampling in the field; Hannah Russ and Harriet White, Bradley Brandt and Sophia Lapidaru, who all ran samples at the University of Sheffield; and Neil Tunstall, Chris Longley, Alison George, Frank Davies and Katheryn Melvin, who assisted with samples at Durham University. Thanks also to Chris Orton and Michele Allan for their assistance with the figures in this chapter.

Supplementary material

For supplementary material related to this chapter, please visit https://doi.org/10.18866/BIAA/e-13. It comprises colour versions of figures 2.2, 2.3, 2.5, 2.6, 2.7, 2.8, 2.9 and 2.11.